

# Comparative study on seismic performance of highly efficient assembled beam-column joints

Panxiong Xu

School of Environment and Architecture, University of Shanghai for Science and Technology, Shanghai

Corresponding Author: Panxiong Xu

---

## Abstract

The assembled beam-column joints are the core bearing parts that affect the seismic performance of the structure. The T-shaped joints and the cross-shaped joints are in different positions of the structure and have different bearing states. In order to study the seismic performance of T-shaped and cross-shaped joints under the same experimental conditions, five full-size models were made, and the low-cycle reciprocating load tests were carried out, and the seismic performance of their hysteretic curves, skeleton curves and displacement ductility were compared. The results show that the beam end bending failure occurs in all the prefabricated joints, but no obvious failure is observed in the composite plates, prefabricated columns and joints. The main failure is the U-shaped through crack near the joint beam end and the bottom of the beam end crushing. There are obvious horizontal shear cracks at the interface between the prefabricated beam and the laminated layer. There is little difference in ultimate bearing capacity, ductility and energy dissipation capacity between the joint with column longitudinal reinforcement and that with column longitudinal reinforcement. The reinforcement structure with column longitudinal reinforcement has little effect on the seismic performance of the joint. The longitudinal bars of the top of each specimen beam are well bonded, and the displacement ductility coefficients of cross joints and T joints have little difference.

**Keywords:** reinforced concrete structure; seismic performance; highly efficient; quasi-static test.

---

Date of Submission: 08-02-2024

Date of acceptance: 23-02-2024

---

## I. INTRODUCTION

Prefabricated concrete buildings have been vigorously promoted due to their advantages such as good production conditions, high construction efficiency and green environmental protection. However, earthquake damage shows that prefabricated beam-column joints are the weak links of structures [1-4]. At the same time, the beam-column joint is the core force part that transmits and distributes the bending moment of the beam-column end. Therefore, many scholars at home and abroad have carried out experimental research on various factors affecting the seismic performance of assembled beam-column joints.

Ma Cailon studied a method of reinforcing bar joint with grout spiral restraint [5]. LUO Xiaoyong conducted a numerical simulation study on the nodes connected by grouting sleeves [6]. Chen Shicai et al conducted a pseudo-static test to compare the beam-pillar-composite plate edge joints and cast-in-place edge joints anchored by reinforcement bolts [7,8]. Zhang Jianxin conducted an experimental study on the beam-column joints using 600MPa grade steel [9]. Zhao Yong did experimental research on assembled columns and middle joints of large-diameter high-strength steel bars [10,11]. The longitudinal bar spacing of the large-diameter and large-spacing high-strength steel beam column joints adopted by Cheng Lu is 468mm[12]. Considering the restraint effect of stirrups on the core area of joints, Qiu Yu conducted experimental research on beam-and-column joints with various stirrups [13].

At present, there are few reports on the seismic performance comparison test of full-size T-type and cross-type beam-column-plate composite under the same test conditions. Although the positions of T-type nodes (middle layer end nodes) and cross-type nodes (middle layer nodes) are different, when seismic loads are imposed on the structure, the connection of the floor makes the displacements of the two nodes coordinate, that is, the horizontal displacements are the same. Therefore, it is necessary to compare the seismic performance of T-shaped joints and cross-shaped joints under the same displacement. In addition, in order to improve the efficiency of assembly construction, the longitudinal reinforcement of prefabricated column is often concentrated in the four corners of the project, and the spacing of longitudinal reinforcement and stirrup limb will be increased. The Technical Standard for Prefabricated Concrete Construction (GB/T 51231-2016) stipulates that the spacing between the longitudinal bars of the prefabricated column should not be greater than 200mm and not greater than 400mm[14]. The seismic performance of the beam-column joints where the longitudinal bars of the prefabricated column are concentrated at four corners is still controversial. In this paper,

a total of five full-size prefabricated joints are designed, and the test variables include axial compression ratio, longitudinal reinforcement arrangement and joint type of prefabricated columns. Pseudo-static test research is carried out to provide test support for seismic design and engineering application of precast concrete buildings.

### 1.1 Experiment design

Five full-size composite beam-plate-prefabricated column joints (including three cruciform joints with numbers J1-3 and two T-shaped joints with numbers J4-5) were made in the test. The upper and lower prefabricated column longitudinal bars of all specimens are connected through the grouting sleeve embedded in the upper column. The top longitudinal bars of the overlapping beam on both sides of the cross-type joint pass through the core area, and the bottom longitudinal bars of the beam are anchored by anchoring plates, while the top longitudinal bars and bottom longitudinal bars of the T-type joint beam are anchored by 90° curved hooks. The column section size is 600mm×600mm, the beam section size is 250mm×500mm, and the plate section size is 110mm×1600mm. The design concrete strength grade of each composite beam and composite plate is C30, and the main reinforcement and stirrup are HRB400E grade reinforcement. The strength grade of precast columns and post-cast concrete in the core area is C50, and the main reinforcement and stirrup are HRB400E grade reinforcement. The reinforcement ratio of each specimen is the same, but the longitudinal reinforcement arrangement of the prefabricated column is different. The longitudinal reinforcement arrangement of J1 and J4 specimens is uniform around the specimens (the longitudinal reinforcement spacing is 163mm), and the longitudinal reinforcement arrangement of J2, J3 and J5 specimens is concentrated in the column (the maximum longitudinal reinforcement spacing is 305mm). In addition, the design axial compression ratio of J3 specimen is 0.37, and the design axial compression ratio of other specimens is 0.25. The main parameters and reinforcement of the specimen are shown in Figure 1.

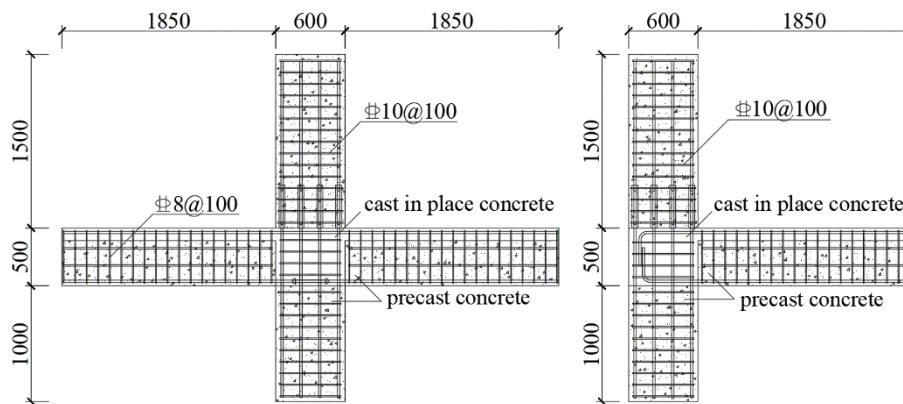


Figure.1 Dimensions of specimens

### 1.2 Experimental loading scheme

The pseudo-static test method was adopted in this test, and the field test equipment was shown in Figure 2. Hinge supports were arranged at the end of the specimen beam and the bottom of the column. The axial pressure was applied to the top of the column by jacks and steel strand, and the horizontal reciprocating load was applied to the top of the column by an actuator. The specific loading process is as follows: first, axial load is applied, then preload is carried out to eliminate the gap between the specimen and the device, and then the displacement is increased step by step. The loading displacement amplitudes were 6, 7.5, 10.5, 15, 22.5, 30, 45, 60, 82.5, 105, 127.5mm, respectively (the corresponding displacement angles were 0.2%, 0.25%, 0.35%, 0.5%, 0.75%, 1%, 1.5%, 2%, 2.75%, 3.5%, 4.25%). Each stage repeats three times. Finally, when the load drops to 85% of the peak load, the specimen is considered to be damaged and the loading is stopped. During the loading process, the horizontal load applied by the actuator is automatically recorded by the actuator, and the displacement at the end of the column is measured by the linear displacement meter.

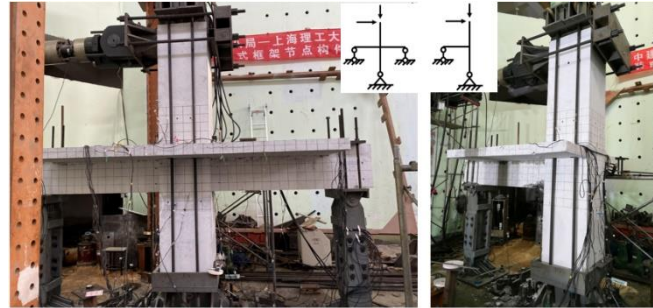


Figure.2 Test setup

## II. RESULT AND DISCUSSION

The results obtained are as discussed below

### 2.1 Failure modes

The five specimens were designed according to "strong column and weak beam", and the crack development and failure characteristics of the specimens were basically similar, and they all experienced four stages of beam end cracking, yield, limit and failure, and the final failure was the yield of the beam end steel bar at the beam-column joint surface. The concrete at the end of the beam is crushed and destroyed, while the concrete in the core area of the joint only appears fracturing phenomenon, and there is obvious sliding phenomenon between the laminated beam and the laminated plate. The failure morphology of each specimen is shown in Figure.3. The failure process of specimen J5 is introduced by taking specimen J5 as an example.

When the specimen is loaded to the horizontal displacement of 6mm, a slight through-vertical crack appears at the bottom of the beam end at the joint plane of the beam column. As the loading continues, the crack at the bottom of the beam expands to the side of the beam, and a new crack appears at the bottom of the beam. When the load reaches the horizontal displacement of 10.5mm, the existing cracks on the beam side develop vertically, and new cracks extend from the bottom of the beam. When the loading reaches the horizontal displacement of 15mm, horizontal cracks appear at the interface between the composite plate and the composite beam, and oblique cracks appear at the interface between the beam plate and the core area. Vertical cracks appear at the interface between the composite plate and the core area, and the cracks extend to the flange of the plate, and the panel near the hinge support has a splay crack. As the loading continues, cracks appear at the joint surface of the beam and the core area, and oblique cracks cross the upper and lower side of the beam, subtle cracks appear in the core area, new cracks grow rapidly, and the original cracks continue to expand and extend. When the horizontal displacement continues to increase, the width of the cracks at the bottom of the beam end near the core area increases rapidly and passes through to the joint surface of the beam and the core area. The vertical cracks near the core area on the laminated plate surface are uniformly distributed, and the splay cracks near the hinge support are dense. When the load reaches the horizontal displacement of 60mm, a small part of the concrete at the bottom of the beam near the core area falls off. When the load reaches the horizontal displacement of 82.5mm, a small part of concrete at the interface of the composite beam and composite plate falls off, and vertical through cracks appear on the side of the beam. When the beam is loaded to the horizontal displacement of 150mm, with the application of reciprocating load, the longitudinal ribs of the beam bottom are raised, the concrete is crushed, a large area falls off, and there are obvious traces of slip between the plate and the beam.

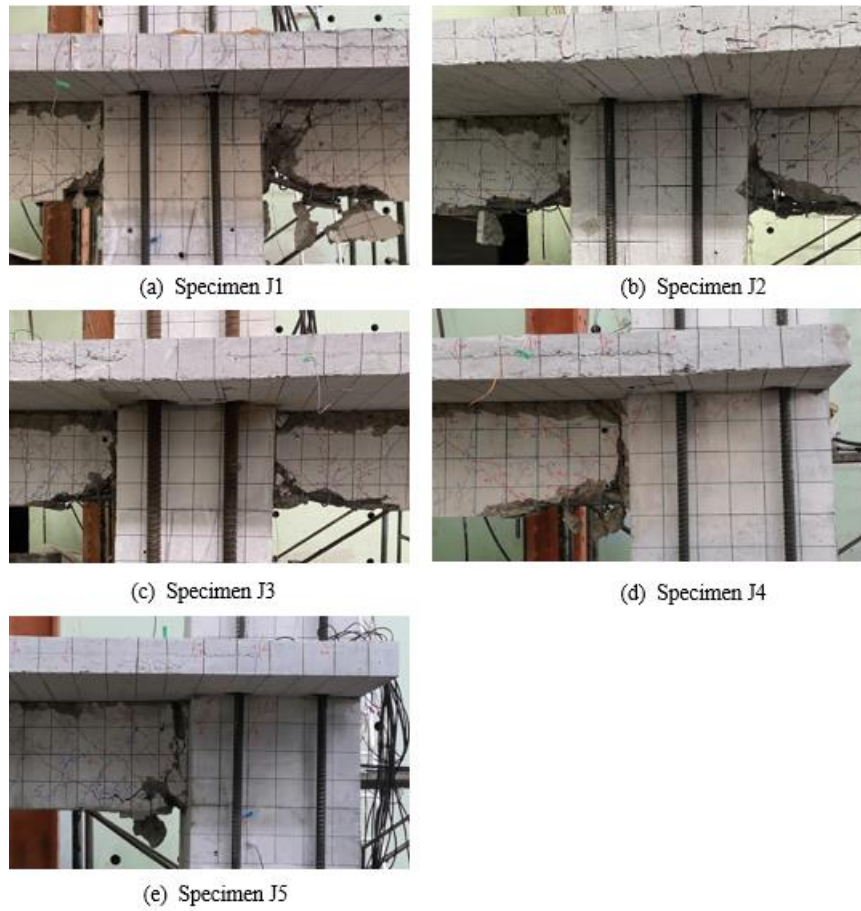


**Figure.4 Failure modes and fractures distribution of specimens**

## **2.2 Hysteretic loops**

Figure.5 shows the hysteretic curves of column top horizontal load and column top horizontal displacement of five specimens. It can be seen from the figure as follows.

(1) Because the composite plate plays the role of the beam flange, the positive and negative loading hysteretic curves of T-shaped nodes are asymmetrical, while the cross-shaped nodes show better symmetry. At the early stage of loading, the stiffness of each specimen is large, the residual deformation is small, and the hysteretic ring is pointed shuttle. With the increase of loading displacement, the concrete cracks to the yield of the steel bar, the residual deformation increases, and the hysteretic ring develops to the arch type. The loading displacement continues to increase, the sliding phenomenon is obvious, the stiffness of the specimen is obviously degraded, and the hysteretic curve shows an inverse S-shape.

(2) The hysteretic curves of J1 and J2 specimens are basically the same, and the hysteretic curves of J4 and J5 specimens are also basically the same, indicating that the longitudinal rib spacing of the magnification column has little influence on the integrity of the joints.

(3) Compared with J2, the hysteretic ring of J3 specimen is more uniform and full, indicating that a high axial compression ratio can improve the hysteretic properties of joints.

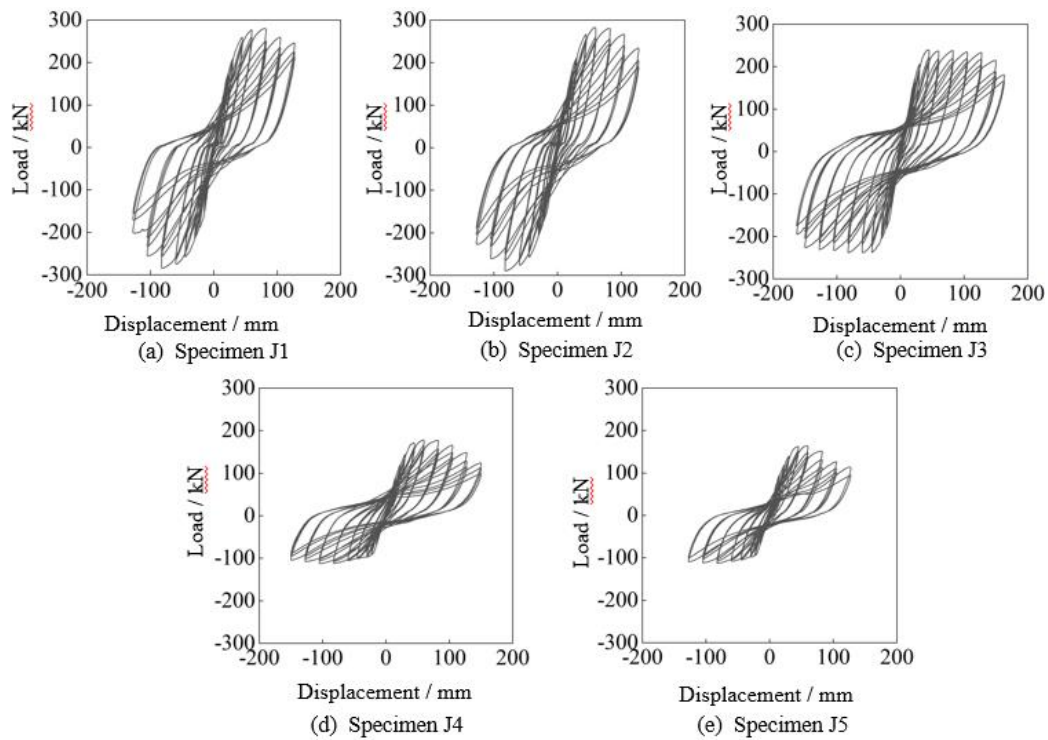


Figure.5 Hysteretic loops of specimens

### 2.3 Skeleton curves

The node skeleton curve is shown in Figure 6 by connecting the peak points of each stage load in the first cycle of each specimen. The test values of characteristic points in the skeleton curve of each specimen are given in Table 1, where the yield load and yield displacement are determined by the energy method, and the displacement ductility coefficient of each specimen is calculated in Table 4, as shown in Figure 6 and Table 4.

(1) The skeleton curves of specimen J1 and J2 are basically identical, and only slightly different in the late period of negative loading, indicating that the magnification of column longitudinal reinforcement spacing has little effect on the bearing capacity of cruciform joints.

(2) Specimen J3 is a large axial compression specific test piece, but in the process of test loading, the concrete at the support of the beam end is crushed, so the fixture of the beam end of specimen J3 has a relatively obvious slip phenomenon, resulting in a small peak load and a large ductility coefficient.

(3) There is little difference between the peak loads of specimen J4 and J5, but in the second half of the forward loading (peak to failure process), the load of specimen J5 decreases slowly, showing better ductility. For the negative loading, the bottom of the beam is strained when the two specimens are damaged, and the load does not decrease significantly, which is mainly due to the yield of the steel bar at the bottom of the beam end. The composite slab concrete has not reached yield, so it can be seen that the negative deformation ability of T-shaped joints is large.

(4) Excluding specimen J3, the displacement ductility coefficient of all specimens is in the range of 2.9~3.4, with the minimum being 2.9 of specimen J2 and the maximum being 3.4 of specimen J5, indicating that all specimens have good ductility.

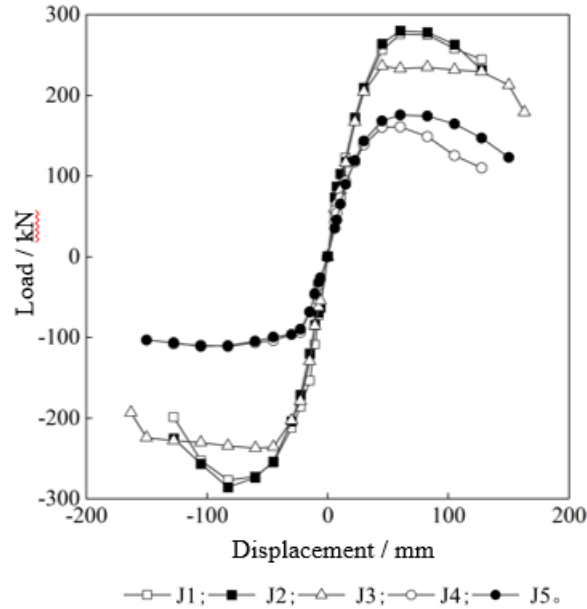


Figure.6 Skeleton curves of specimens

Table 1: Displacement ductility coefficient of specimens.

Jointss	Yield Points		Fail Points		Ductility Factors $\mu$
	$P_y/kN$	$\Delta_y/mm$	$P_u/kN$	$\Delta_u/mm$	
J1	243.4	41.2	237.9	138.8	3.4
	-231.1	-36.6	-241.6	-109.6	3.0
J2	244.0	39.6	240.6	121.3	3.1
	-253.7	-38.4	-245.9	-112.7	2.9
J3	211.0	33.2	203.5	153.6	4.6
	-208.5	-32.5	-202.6	-159.2	4.9
J4	139.9	31.0	139.4	91.7	3.0
	-97.5	-32.8	—	—	
J5	153.5	36.3	151.2	122.5	3.4
	-97.6	-35.6	—	—	

### III. CONCLUSION

1) Beam end bending failure occurred in all assembled joints, but no obvious failure was observed in composite plates, prefabricated columns and joints, and the failure was mainly caused by longitudinal reinforcement buckling near the bottom of the joint beam end and concrete crushing at the bottom of the beam end.

2) There is little difference in ultimate bearing capacity, ductility and energy dissipation capacity between the joint with centralized longitudinal reinforcement and the joint with uniform longitudinal reinforcement, and the reinforcement structure with centralized longitudinal reinforcement has little influence on the seismic performance of the joint.

3) Due to the slip cracks at the interface between the prefabricated beam and the laminated layer, the longitudinal bars of the top of each specimen beam are well bonded, and the displacement ductility coefficients of the cross-shaped joints and T-shaped joints are not much different.

## REFERENCES

- [1]. SAVOIA M; BURATTI N; VINCENZI L. (2017). "Damage and collapses in industrial precast buildings after the 2012 Emilia earthquake" *Engineering Structures*, 137: 162-180.
- [2]. WU Gang, FENG Decheng. (2018) "Research progress on fundamental performance of precast concrete frame beam-to-column connections" *Journal of Building Structures*, 39(2):1-16.
- [3]. YAN Xikang, XIE Hanlin, LIANG Linxiao, et al. (2003)"Effect of splicing on seismic performance of prefabricated RC structural nodes" *Journal of Architecture and Civil Engineering*,40(1): 85-94.
- [4]. GUAN Dongzhi, JIANG Cheng, GUO Zhengxing, et al. (2018) "Development and seismic behavior of precast concrete beam-to-column connections" *Journal of Earthquake Engineering*, 22(2): 234-256.
- [5]. MA C L, JIANG H, WANG Z Y. (2019) "Experimental investigation of precast RC interior beam-column-slab joints with grouted spiral-confined lap connection" *Engineering Structures*, 196: 109317.
- [6]. LUO Xiaoyong, LONG Hao, OU Ya, et al. (2021), "Study on finite element model of the prefabricated reinforced concrete beam-column joints with grouted sleeves" *Advances in Civil Engineering*,2021:1-15.
- [7]. CHEN Shicai, YAN Weiming, WANG Wenming , et al. (2011) "Seismic behavior of exterior beam to column joints with layered slab of large precast concrete constructures" *Journal of Building Structures*, 6: 60-67.
- [8]. YAN Weiming, WANG Wenming, CHEN Shicai, et al. (2010) "Experimental study of the seismic behavior of precast concrete layered slab and beam to column exterior joints" *Journal of Building Structures*, 12:56-61.
- [9]. ZHANG J X, RONG X, WU H C. (2017), "Experimental research on hysteretic behavior of exterior joints with 600 megapascal reinforced bars" *Industrial Construction*, 47(6): 30-33.
- [10]. ZHAO Yong, LI Rui, WANG Xiaofeng, et al.(2017) "Experimental research on seismic behaviors of precast concrete columns with large-diameter and high-yield strength reinforcements splicing by grout-filled coupling sleeves" *China Civil Engineering Journal*, 50(5): 27-35.
- [11]. ZHAO Yong, SHI Lin, TIAN Chunyu, et al.(2021) "Experimental study on seismic performance of beam-column sub-assembly in monolithic precast concrete frame" *Journal of Building Structures*, 42:133-143.
- [12]. LIU Lu, HUANG Xiaokun, TIAN Chunyu, et al.(2016) "Experimental study on seismic performance of precast RC frame joints with HRB500 high strength rebars of large diameter and spacing" *Journal of Building Structures*,37(5): 247-254.
- [13]. QIU Y, ZHOU X Z, LUO Y H, et al.(2022) "Research on seismic performance of prefabricated concrete beam-to-column joints with new stirrups" *Industrial Construction*, 52(12): 72-79.
- [14]. China Architecture & Building Press. (2016) "China Institute of Building Standard Design & Research. Technical standard for assembled buildings with concrete structure: GB/T 51231-2016" Beijing.